中正嶺學報 第三十四卷 第二期 民國 95.5.
JOURNAL OF C.C.I.T., VOL.34, NO.2, May., 2006

The Optimum Characteristics for the Fiber Coupled Laser Diode End-Pumped Lasers

Kun-Fu Tseng* and Yung-Sheng Huang**

**Department of Electronic Engineering*
Chin-Min Institute of Technology
***Department of Electrical Engineering*
I-Shou University

ABSTRACT

In this paper, we have included the absorption coefficient and finite laser rod length into the analysis of the optimization of the fiber coupled laser–diode end–pumped laser. From the numerical results, we obtain an analytic solution to explain the required input power and the pumped beam quality to the laser output power of an active laser medium. For different kinds of the laser media which correspond to different absorption coefficients with given laser rod lengths will produce different optimum pump beam qualities and different output efficiencies. Some phenomena are shown and discussed in this article.

Keywords: fiber coupled diode-end –pumped laser, absorption coefficient, mode size optimization

光纖耦合雷射二極體端點激發雷射之最佳化條件

曾昆福* 黃永生**

*親民技術學院 電子工程系

**義守大學 電機工程系

摘 要

本文將不同雷射材料之吸收參數及長度，納入光纖耦合雷射二極體端點激發雷射之最佳化條件中計算，由分析結果中我們獲得一個解析解，可計算出要獲得一理想的雷射輸出功率所需的輸入功率及激發光束的相關品質因素。不同的雷射材料有不同的吸收係數，對不同的材料之吸收係數及長度所對應理想化的光束品質及光輸出效率，本文中有許多結果呈現並加以討論。

關鍵字: 光纖耦合雷射二極體端點激發雷射、吸收常數、模數大小理想化

文稿收件日期 93.10.19; 文稿修正後接受日期 94.8.25.
Manuscript received October 19, 2004; revised August 25, 2005.

Ⅰ. INTRODUCTION

Laser diode (LD)-pumped solid-state lasers have wide applications for their high efficiency, simplicity, compactness, good frequency stability, and high beam quality, etc. Since the early 1980's with the development of reliable high power LD, the LD-pumped solid-state lasers had received much attention, especially in the end-pumping configuration [1-4]. P. Laporta and M. Brussard proposed a general formulism about the design and optimization criteria for mode size optimization in diode-pumped solid-state lasers [5]. Base on this model, Y.F. Chen et al. gave a simple analytical expression for the fiber-coupled laser diode end-pumped lasers including the effect of pump beam quality into the analysis [6,7]. Under these optimum pump conditions, experimental results had shown that the green laser output power corresponded to high conversion efficiency [8].

Theoretical and experimental results showed that the maximum laser output for end-pumped solid-state laser was limited by thermal fracture of the laser crystal [9-12]. Also the fracture-limited pump power for an end-pumped solid-state laser was strongly dependent on the absorption coefficient. The same doping concentration in different crystals could have different absorption coefficients under a given pump wavelength (such as, Nd: YAG and Nd: YOV_4). A high absorption coefficient could lead to high slope efficiency for the TEM_{00} mode. Nevertheless, it could result in a large temperature gradient in the pump end of the crystal which could result larger thermal loading and produce thermal fracture, consequently [13].

In this paper, we apply a numerical method to calculate the optimization of the pump beam quality, including the pump beam waist, the far-field half-angle , the focal plane of the pump beam in the active medium, the minimized average pump spot size and the output power at the condition of minimum average pump size. These optimum parameters enable us to design the laser resonator and the optical coupling system for optimization. They also provide a guideline to choice the best laser medium length. To illustrate the utility of the present model, two kinds of the laser media SDL-2372-P2 and SDL-2372-P3 [6] are chosen to compare.

Ⅱ. MODEL

Figure 1 is a configuration of diode-pumped solid-state lasers. In this system, a laser diode array emits input light coupled to a laser medium rod with a length L, and then reaches to the reflective mirror. The W_P and W_l are the pump beam waist and the beam waist of the laser cavity, respectively.

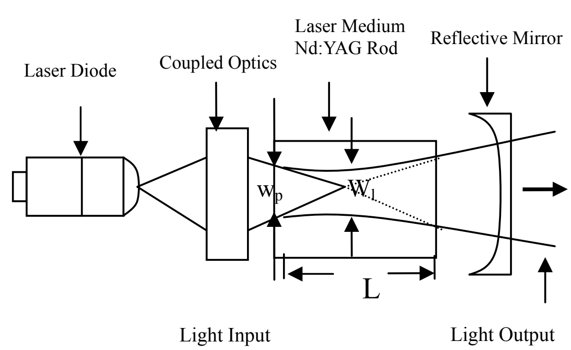

Fig. 1. A configuration of diode-pumped solid-state lasers.

Laporta and Brussard have used the space-dependent rate equation to develop the general design criteria for mode size optimization in diode-pumped solid-state lasers [5]. In his model, the average pump beam waist $\overline{W}_p$ is assumed a constant when the far-field half-angle $\theta_p \le 0.2$ rad. The average pump beam size is expressed as [5]:

$$\overline{W}_p = \left[\frac{1}{l^*} \int_0^{l^*} \omega_p^2(z) dz \right]^{1/2} \tag{1}$$

where l^* is a suitable effective length related to the absorption length of the pump radiation, and it can be described as the following equation:

$$l^* = (-2.3\theta_p + 1.8)(1/\alpha) \tag{2}$$

where α is the absorption coefficient of the laser rod. It gives a good approximation to evaluate the overlap integral. For a fiber-coupled pump beam $r_p(r,z)$ traveling along the optical axis z-axis can be expressed as

$$r_p(r,z) = \frac{2\alpha}{\pi \overline{W}_p^2(z)\left(1-\exp(-\alpha L)\right)} \times \exp(-2\frac{r^2}{\overline{W}_p^2(z)} - \alpha z) \tag{3}$$

where L is the length of laser rod. Under plane wave approximation and through a linearization procedure, the output power can be expressed as a function a normalization parameter χ

$$P_{out} = \frac{T\eta_p}{2\gamma} \frac{(\frac{W_{l0}}{\overline{W}_p})^2[(\frac{W_{l0}}{\overline{W}_p})^2 + 2]}{[1+(\frac{W_{l0}}{\overline{W}_p})^2]^2} \times P_{in}[1 - \frac{(W_{l0}{}^2 + \overline{W}_p^2)}{\chi}] \tag{4}$$

where $$\chi \equiv \frac{P_{in}}{(\pi\gamma I_{sat}/2\eta_p)} \tag{5}$$

The threshold pump power is

$$P_{th} = \frac{\pi\gamma I_{sat}}{2\eta_p}(W_{l0}^2 + \overline{W}_p^2) \tag{6}$$

In Eq. (4), W_{lo} is the beam waist of the laser cavity mode and T is the power transmission of the output coupler. The pumping efficiency η_p is equal to $\eta_t\eta_a(\nu_l/\nu_p)$, which is the product of the optical transfer efficiency η_t, (the ratio of the optical power which incidents into the active medium and the emitted power by the pump source), and η_a the absorption efficiency (the ratio of the power which is absorbed in the active medium and the power enters the rod), and the ratio of the laser frequency υ_l with pumping frequency υ_p. The γ is the total logarithmic loss per pass. The I_{sat} in Eq. (5) represents the saturation intensity.

From Eq. (4) and Eq. (6), it shows that the smaller pump beam waist $\overline{W}_p$ leads to a smaller threshold pump power P_{th} and larger slope efficiency. Thus, it can be used in determining the minimized value of the pump beam waist $\overline{W}_p$ for a given pump beam quality and properties of the active medium. On the basis of the paraxial approximation, Chen et al. suggest that the average pump beam waist $\overline{W}_p$ is expressed as [7]

$$\overline{W}_p = \frac{\int_0^L [W_{p0} + (\frac{c}{nW_{p0}})\left|Z - Z_0\right|]e^{-\alpha Z} dZ}{\int_0^L e^{-\alpha Z} dZ} \tag{7}$$

where the W_{po} is the radius at the waist, and the weight function $e^{-\alpha z}$ comes from the absorption effect (the light comes from the optical fiber and couples into the laser rod). In common situations, the incident light is assumed to be totally absorbed by the medium, but in fact it is related to many operation parameters, including the far field angle and the beam quality, etc. Eq. (7) used in their work [7] which is consistent with Eq. (1). The relationship between W_{po}, θ_p and z_0 is given by [14]

$$W_p(z) = W_{p0} + \theta_p \left| Z - Z_0 \right| \tag{8}$$

The θ_p and Z_0 are the far-field half-angle and the focal plane of the pump beam in the active medium, respectively. From Eq. (8), the pump beam waist $W_p(z)$ is a function of divergence of far-field angle and the focal position in the active medium. It is satisfied with beams and partial spatial coherence.

Starting from Eq. (7), the integrand can be integrated exactly. We perform this integral to determine the optimized focal plane position $Z_{0,opt}$ and the minimum radius at the waist $W_{p0,opt}$. Both are expressed as following

$$Z_{0,opt} = \frac{1}{\alpha}\ln\left(\frac{2}{1+e^{-\alpha L}}\right) \tag{9}$$

and

$$W_{p0,opt} = \frac{1}{\alpha}\sqrt{\frac{c}{n}}\frac{1}{\sqrt{1-e^{-\alpha L}}}\left[(1+e^{-\alpha L})\ln\left(\frac{2}{1+e^{-\alpha L}}\right) - \alpha L e^{-\alpha L}\right]^{\frac{1}{2}} \tag{10}$$

where c is the characteristic of LD pump beam quality and n is the refractive index in the laser rod.

Considering Eq. (9), the optimized focal plane position $Z_{0,opt}$ is dependent on the factor $\ln\left(\frac{2}{1+e^{-\alpha L}}\right)$ and is inversely proportional to the absorption coefficient α. On the other hand, if the entering light is not absorbed by the active medium entirely, we must consider a correction factor which depends on the product of α and L. Note that the larger α makes the optimized focal plane position closer to the incident surface in the active medium.

In the limit case, $\alpha L \approx \infty$, then Eq. (9) and Eq. (10) become

$$Z_{0,opt} = \frac{1}{\alpha}\ln(2) \tag{11}$$

and

$$W_{p0,opt} = \frac{1}{\alpha}\sqrt{\frac{c}{n}}\sqrt{\ln 2} \text{ , respectively.} \tag{12}$$

Substituting Eq. (9) and Eq. (10) into Eq. (7), we obtain the minimum value of the pump beam waist $\overline{W}_p$ for a given pump beam quality

$$\overline{W}_{p,\min} = \frac{2}{\alpha}\sqrt{\frac{c}{n}}\frac{1}{\sqrt{1-e^{-\alpha L}}}\left[(1+e^{-\alpha L})\ln\frac{2}{1+e^{-\alpha L}} - \alpha L e^{-\alpha L}\right]^{\frac{1}{2}} \tag{13}$$

If $\alpha L \approx \infty$, then Eq. (13) becomes

$$\overline{W}_{p,\min} = \frac{2}{\alpha}\sqrt{\frac{c}{n}}\sqrt{\ln 2} \tag{14}$$

Eq. (13) allows us to determine the optimized far-field half-angle θ_p [14] as

$$\theta_{p0,opt} = \frac{c}{nW_{p0}}\Big|_{W_{p0,opt}} = \alpha\sqrt{\frac{c}{n}}\sqrt{1-e^{-\alpha L}} \times \left[(1+e^{-\alpha L})\ln\frac{2}{1+e^{-\alpha L}} - \alpha L e^{-\alpha L}\right]^{\frac{-1}{2}}. \tag{15}$$

If $\alpha L \approx \infty$, then

$$\theta_{p0,opt} = \alpha\sqrt{\frac{c}{n\ln 2}} \tag{16}$$

The Eq. (9) ~ Eq. (16) are all simple analytic expressions for design the optical pump beam coupling system and they are also related to the pump beam quality in the active medium (i.e., α, n and c).

The condition for determining the optimum mode size and the maximum output power is through

$$\frac{\partial P_{out}}{\partial W_{l0}} = 0 \cdot \tag{17}$$

This equation leads to an analytic numerical solution of the optimum W_{lo},

$$W_{10,opt} = \frac{1}{\sqrt{3}}[3^{1/3}\frac{\overline{W}_{p,\min}}{C_3} f(\overline{W}_p, \frac{\gamma I_{sat}}{\eta_p}, P_{in}) - \frac{3^{2/3}\overline{W}^3_{p,\min} C_3}{f(\overline{W}_{p,\min}, \frac{\gamma I_{sat}}{\eta_p}, P_{in})} - 3\overline{W}^2_{p,\min}]^{1/2} \tag{18}$$

where

$$f(\overline{W}_p, \frac{\gamma \cdot I_{sat}}{\eta_p}, P_{in}) = C_2^{1/3} C_3^{2/3} (9P_{in} + \sqrt{3}\sqrt{C_3^2 C_2^4 + 27P_{in}^2})^{1/3} \cdot \tag{19}$$

The coefficients C_2, and C_3 in Eq. (19) are defined as

$$C_2 = \overline{W}_{p,\min} \tag{20}$$

and

$$C_3 = \frac{\pi\gamma I_{sat}}{2\eta_p} \cdot \tag{21}$$

The Eq. (18) can offer us how to design a laser resonator cavity. The function $f(\overline{W}_p, \frac{\gamma I_{sat}}{\eta_p}, P_{in})$ is defined in Eq. (19). When the optimum mode size $W_{lo,opt}$ and the laser resonator cavity for the maximum output power are determined. Substituting Eq. (18)~ Eq. (21), and Eq. (12) into the Eq. (4) and Eq. (5), respectively. We can obtain the maximum output power and the output efficiency which are expressed as following

$$P_{out} = \frac{1}{8}\frac{T\eta W_{l0}^2\alpha^2 n}{\gamma c \ln 2}\frac{\frac{W_{l0}^2\alpha^2 n}{4c\ln 2}+2}{\frac{W_{l0}^2\alpha^2 n}{4c\ln 2}+1}[P_{in} - \frac{1}{2}\frac{\pi\gamma I_{sat}(W_{l0}^2 + \frac{4c\ln 2}{\alpha^2 n})}{\eta}] \tag{22}$$

and

$$\sigma_{\max} = (\frac{P_{\max}}{P_{in}})/(\frac{T\eta_p}{2\gamma}) = \frac{(\frac{W_{l0}}{W_p})^2[(\frac{W_{l0}}{W_p})^2+2]}{[1+(\frac{W_{l0}}{W_p})^2]^2} \times (1 - \frac{W_{l0}^2 + W_p^2}{\chi}) \tag{23}$$

, respectively.

Ⅲ. NUMERICAL SIMULATION

We have considered a Nd : YAG laser end-pumped by a diode-laser as a design example and used the following parameters : $I_{sat} = 2.32 \times 10^4 (\text{mW/mm}^2)$, $\gamma = 0.028$ (output coupling $T = 0.05$ and internal loss per transit is 0.003), and $\eta_p = 0.67$, it is found that the ratio between input power and pump beam quality is always larger than $2.12 \times 10^4 (\text{mW/mm} \cdot \text{rad})$ and will obtain an output efficiency higher than 30% [7]. In this paper, the laser diodes SDL-2372-P2 and SDL-2372-P3 are used to research. The schematic diagram of laser setup is as Fig. 1.

From Spectra Diode Laboratories and Chen et al. [6], the laser diodes' quality factors SDL-2372-P2 and SDL-2372-P3 are $c_{p2} = 0.05568$ and $c_{p3} = 0.02016$, respectively. SDL-2372-P2 has a 200-μm-core fiber of a ~36^{o} half width at e^{-2} maximum and SDL-2372-P3 has a 100-μm-core fiber of a ~26° half width at e^{-2} maximum. The brightness of model SDL-2372-P3 is three times as much as that of model SDL-2372-P2. Both have the same maximum CW power input $P_{in.\max} = 1200\text{mW}$. The refractive index $n = 1.2$ is used in the active medium for a given pumping wavelength.

Figure 2 shows that $Z_{0,opt}$ as a function of absorption coefficient α for different lengths of laser rods, it is calculated by Eq. (9).

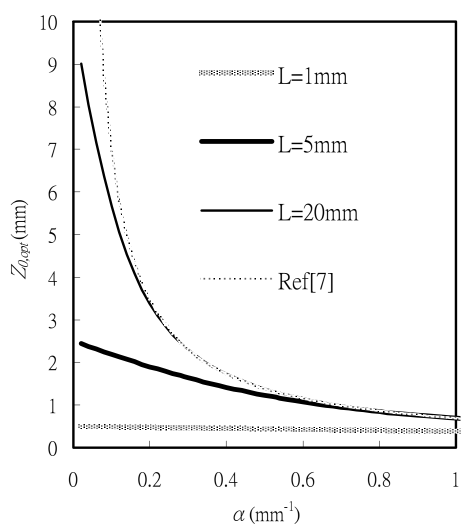

Fig. 2. The optimum focal plane as a function of absorption coefficient for several different lengths of laser rod.

Figure 3 predicts the theoretical results of Nd: YAG output power versus Z_0 calculated from Eq. (8)- Eq. (12), Eq. (18) - Eq. (22) and its relative parameters, The experimental results of output power versus Z_0 are shown in Fig. 4. Chen et al. predict the optimum focal plane $Z_{0,opt}$ is 1.16 mm [7], but the $Z_{0,opt}$ is about 1.08 mm comparing with ours. Both of the values are close to the experimental data, and it is about a 7% of difference. The difference between both models is that we have taken the factors of the finite length of the rod L and its absorption coefficient α into consideration. The other uses the combined factors of β and χ, where β is equal to C/nα and χ is defined as Eq. (5). From the definition of parameters, it is easy to understand the advantage of our model.

Figure 5 shows the pump beam quality $W_{po,opt}$ vs. α in different lengths of laser rods from Eq. (10). Minimum pump beam waist $W_{p,\min}$ vs. α in different laser rod lengths from Eq. (13) are shown in Fig. 6. Laporta and Bussard have pointed out that a smaller $\overline{W}_p$ can lead to a smaller threshold pump power and larger slope efficiency [5]. Thus it is useful to determine the minimum of $W_{p,\min}$ vs. α from Eq. (13). From Fig. 6 and Fig. 7, it is clear when α is approached to small value, the value of $W_{po\cdot opt}$ and $W_{p\cdot\min}$ are quite different under different lengths of laser rods.

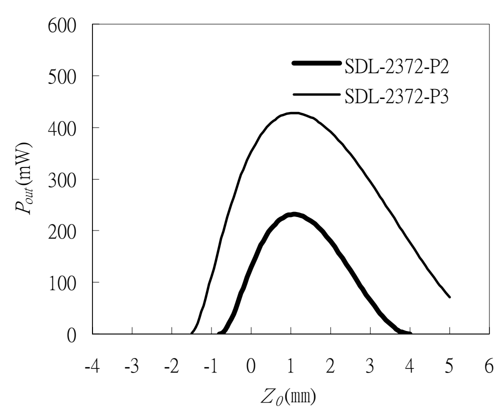

Fig. 3. Theoretical prediction of Nd: YAG output power versus the depth of focus inside the rod.

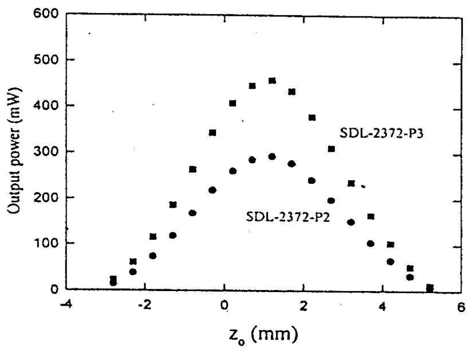

Fig. 4. Experimental results of output power pumped versus depth of focus inside the rod at 1.15W pump power. (Data source come from [7])

However, we find it needs more consideration on the effect of finite length of laser rod L and the product of value αL. The choice of active medium of laser rod which gives a different absorption coefficient will result a different pump beam quality. Therefore, the equations from Eq. (10) to Eq. (15) can be used as a reference to design a pump beam quality.

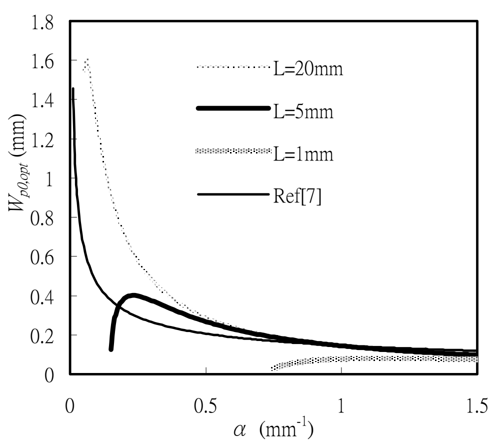

Fig. 5. The optimum radium at the waist as a function of absorption coefficient for several different lengths of laser rod.

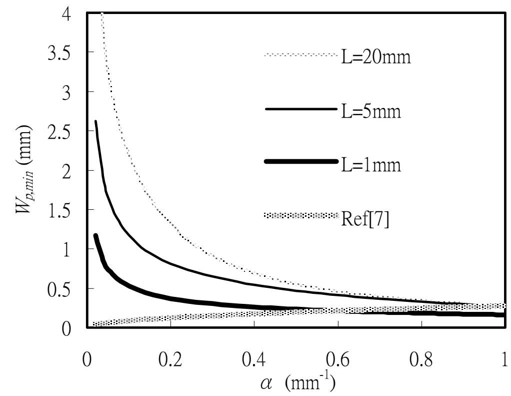

Fig. 6. The minimum pump beam waist as a function of absorption coefficient for several different lengths of rods.

Figure 7 shows the results of $\theta_{p0\cdot opt}$ versus α from Eq. (15). It is important to determine the ratios of W_{l0}/W_{p0} which affect the laser output power of the optical system. Some articles point out that a larger length of active medium L is needed for a lower absorption coefficient α. It is assumed that the entering pump light into the active medium would be absorbed entirely, but it is always some loss actually.

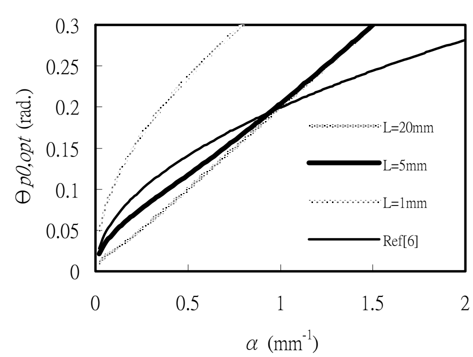

Fig. 7. The optimum far field half angle as a function of absorption coefficient for several different lengths of laser rod.

Figure 8 shows that an optimum laser mode size $W_{l0,opt}$ depends not only on α but also L. It means that we can get the $W_{l0,opt}$ by adjusting the parameters α and L. Fig. 9 shows the numerical simulation results as Eq. (4) is used for calculation. The curves of the normalized output power P_{out} versus the normalized pump power P_{in} are shown. It is found from Eq. (6) that a larger ratio of $W_{l0}/\overline{W}_{p0}$ will result in a larger threshold pump power, but it cannot get a larger slope efficiency and output power as shown in Fig. 9. Only when the optimum ratio $W_{l0}/\overline{W}_{p0}$ is controlled, it may obtain the maximum output power. Two different active media SDL-2372-P2 and SDL-2372-P3 [6] are taken for comparison.

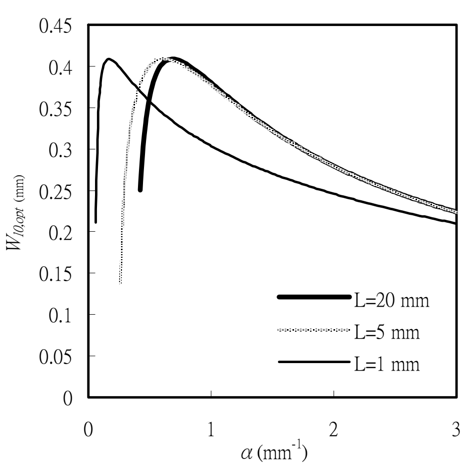

Fig. 8. The optimum laser mode size as a function of absorption coefficient for several different lengths of laser rod.

Figure 10 shows the output power as a function of the pump power, in which Eq. (22) is used. Our calculations are quantitative satisfied and very agreement with the experimental results shown in Fig. 11. The comparison of the numerical data differences between ours and [7] models are shown in Table 1.

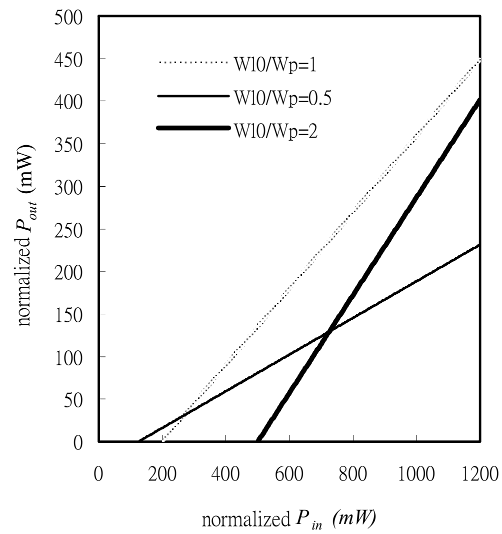

Fig. 9. Normalized output power as a function of the normalized input power for several ratios of the mode to pump spot size.

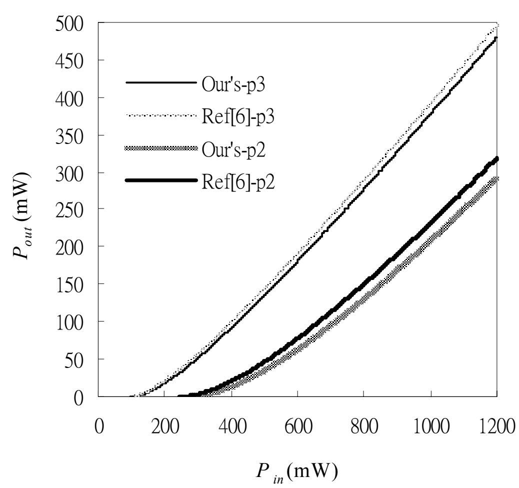

Fig. 10. Theoretical prediction of the Nd:YAG output power versus fiber coupled pump power. The graphics show that a quantitative difference in the two modes.

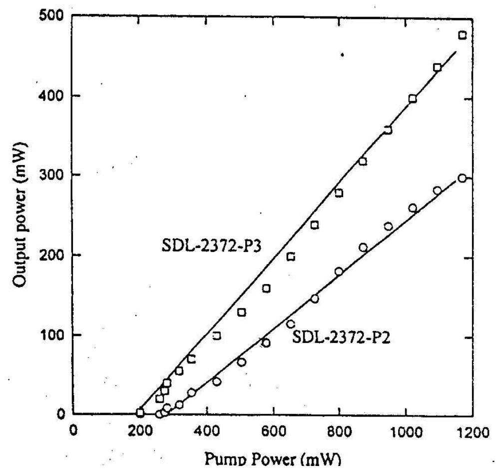

Fig. 11. Experimental results of the Nd:YAG output power versus pump power. (Data from [6],[7])

Table 1. The comparison of the numerical difference of both ours and [7] models

LD Type	$Z_{0,opt}$ (mm)		$W_{l0,opt}$ (mm)		σ_{max} (%)	
	This work	Ref. [7]	This work	Ref. [7]	This work	Ref. [7]
SDL-2372-P2	1.08	1.16	0.40	0.36	41	50
SDL-2372-P3	1.08	1.16	0.34	0.32	67	70

Our results in the last column of Table 1, the maximum output efficiency σ_{max} are approximately 41% and 67% for SDL-2372-P2 and SDL-2372-P3, respectively. Comparing with other model [6,7], it shows that there are some quantitative differences between these two models, but they are close to each other. Fig. 12 shows the theoretical curves of the maximum output efficiency as a function of the mode spot size, which are calculated from Eq. (23).

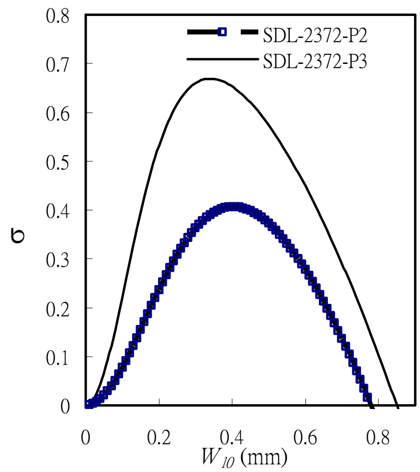

Fig. 12. Theoretical prediction of the maximum output efficiency as a function of mode spot size.

Ⅳ. CONCLUSIONS

We have given a simple expression for design the optimization of the fiber-coupled laser diode pumped laser. The numerical results show that the optimum parameters are related with the pump spot size, laser mode size, and the pump beam quality. Our model takes the parameters of absorption coefficient and length of laser rod into consideration, which can provide a straightforward procedure to design the laser cavity resonator and the optical coupling system for maximum the output power. And it also offers a useful reference to choice the pump source and active medium parameters.

REFERENCES

[1] Chen, Y. F., Lan, Y. P., and Wang, S. C., "Influence of Energy-Transfer Upconversion on the Performance of High Power Diode-Pumped CW Laser," IEEE J. Quantum Electronics, Vol. 36, No. 5, pp. 615-619, 2000.

[2] Blows, J. L., Omatsu, T., Dawes, J., Pask, H., and Tateda, M., "Heat Generation in Nd:YVO_4 with and without Laser Action," IEEE Photonics Tech. Lett., Vol. 10, No. 12, pp. 1727-1729, 1998.

[3] Hardman, P. J., Clarkson, W. A., Friel, G. J., Pollnau, M., and Hanna, D. C., "Energy Transfer Upconversion and Thermal Lensing in High Power End-Pumped Nd:YLF Laser Crystals," IEEE J. Quantum Electronics, Vol. 35, No. 4, pp. 647-655, 1999.

[4] Zhang, X., Zhao, S., Wang, Q., Ozygus, B., and Weber, "Modeling of Diode-Pumped Actively Q-Switched Lasers," IEEE J. Quantum Electronics, Vol. 35, No. 12, pp. 1912-1918, 1999.

[5] Laporta, P. and Brussard, M., "Design Criteria for Mode Size Optimization in Diode Pumped Solid-State Lasers," IEEE J. Quantum Electronics, Vol. 27, No. 10, pp. 2319-2326, 1991.

[6] Chen, Y. F., "Optimization of Fiber-Coupled Laser–Diode End-Pumped Lasers: Influence of Pump-Beam Quality," IEEE J. Quantum Electronics, Vol. 32, No. 11, pp. 2010-2016, 1996.

[7] Chen, Y. F., "Analytical Model for the Design of Fiber-Coupled Laser-Diode End-Pumped Laser," Optics Communications Vol. 133, No. 6, pp. 517-524, 1997.

[8] Chen, Y. F., Wang, S. C., Kao, C. F., and Haung, T. M., "Investigation of Fiber-Coupled Laser Diode-Pumped NYAB Green Laser Performance," IEEE Photonics Tech. Lett., Vol. 8, No. 10, pp. 1313-1315, 1996.

[9] Tsunekane, M. and Taguchi N., "Analytical and Experimental Studies on the Characteristics of Composite Solid-State Laser Rods in Diode-End-Pumped Geometry," IEEE J. Select. Topics Quantum Electron, Vol. 3, No. 1, pp. 9-18, 1997.

[10] Tidwell, S. C., Seamans, J. F., Bowers, M. S., and Cousiins, A. K., "Scaling CW Diode-End-Pumped Nd-YAG Lasers to High Average Powers," IEEE J. Quantum Electron, Vol. 28, No. 4, pp. 997-1009, 1992.

[11] Sasaki, T. and Kojima, T., "Single-Longitudinal-Mode Operation and Second-Harmonic Generation of Nd : YVO_4 Microchip Lasers," Optical. Letters. Vol. 16, No. 21, pp. 1665-1667, 1991.

[12] Cousins, A. K., "Temperature and Thermal Stress Scaling in Finite-Length End-Pump Laser Rods," IEEE J. Quantum Electron, Vol. 28, No. 4, pp. 1057-1069, 1992.

[13] Chen, Y. F., "Design Criteria for Concentration Optimization in Scaling Diode End-Pumped Lasers to High Powers: Influence of Thermal Fracture," IEEE J. Quantum Electronics, Vol. 35, No. 2, pp. 234-239, 1999.

[14] Fan, T. Y. and Sanchez, A., "Pump Source Requirements for End-Pumped Lasers," IEEE J. Quantum Electronics, Vol. 26, No. 2, pp. 311-316, 1990.